Contents lists available at ScienceDirect

Colloids and Surfaces B: Biointerfaces

PEG-b-poly (carbonate)-derived nanocarrier platform with pH-responsive properties for pancreatic cancer combination therapy

Priyanka Ray[a], Matthew Confeld[b], Pawel Borowicz[c], Tao Wang[d], Sanku Mallik[b,**], Mohiuddin Quadir[a,*]

[a] *Department of Coatings and Polymeric Materials, North Dakota State University, Fargo, ND, USA*
[b] *Department of Pharmaceutical Sciences, North Dakota State University, Fargo, ND, USA*
[c] *Department of Animal Sciences, North Dakota State University, Fargo, ND, USA*
[d] *Core Biology Facility, North Dakota State University, Fargo, ND, USA*

ABSTRACT

A pH-responsive nanoparticle platform, based on PEG-b-poly (carbonate) block copolymers have been proposed that can respond to low pH as found in many cancer micro- and intracellular environment, including that in pancreatic cancer. The hydrophobic domain, *i.e.*, the poly (carbonate) segment has been substituted with tertiary amine side chains, such as N, N'-dibutylethylenediamine (pK_a = 4.0, DB) and 2-pyrrolidin-1-yl-ethyl-amine (pk_a = 5.4, Py) to generate two different sets of block copolymers namely PEG-DB and PEG-PY systems. These side-chain appended amines promote disassembly of nanoparticles and activation of drug release in response to pH conditions mimicking extra- (pH 6.9–6.5) and intracellular compartments (5.5–4.5, from early endosome to lysosome) of cancer tissues respectively. A frontline chemotherapy used for pancreatic cancer, *i.e.*, gemcitabine (GEM) and a Hedgehog inhibitor (GDC 0449) has been used as the model combination to evaluate the encapsulation and pH-dependent release efficiency of these block copolymers. We found that, depending on the tertiary amine side chains appended to the polycarbonate segment, these block copolymers self-assemble to form nanoparticles with the size range of 100–150 nm (with a critical association concentration value in the order of 10^{-6} M). We also demonstrated an approach where GEM and GDC 0449-encapsulated PEG-DB and PEG-PY nanoparticles, responsive to two different pH conditions, when mixed at a 1:1 vol ratio, yielded a pH-dependent co-release of the encapsulated contents. We envision that such release behaviour can be exploited to gain spatiotemporal control over drug accumulation in pathological compartments with different pH status. The mixture of pH-responsive nanoparticles was found to suppress pancreatic cancer cell proliferation when loaded with anticancer agents *in vitro*. Cell-proliferation assay showed that both variants of PEG-b-polycarbonate block copolymers were inherently non-toxic. We have also immobilized iRGD peptide on intracellularly activable PEG-DB systems to augment cellular uptake. These targeted nanoparticles were found to promote selective internalization of particles in pancreatic cancer cells and tumor tissue.

1. Introduction

A large cohort of clinical conditions, ranging from inflammation to cancer, precipitates in pH-differentials existing across different pathophysiological compartments of the disease-microenvironment [1–3]. Pancreatic Ductal Adenocarcinoma (PDAC) for example, is one of such diseases and is the most virulent forms of all cancers which shows a prominent gradient of decreasing pH from extracellular to intracellular compartments [4]. Clinical success of PDAC critically hinges on addressing a set of mutually connected, yet compartmentalized, pathology that includes mature and differentiated cancer cells in an acidified (as low as pH 6.0–6.5, for pancreatic cancer), desmoplasia-protected microenvironment. While desmoplasia impairs the delivery of drugs to malignant cells of this disease, tumor-stroma interaction of paracrine or autocrine origin, create a complicated signaling network in PDAC that drives tumor progression and prognosis [5,6]. Hence, combination therapy, such as gemcitabine (GEM, an antimetabolite, active in the nucleus) and a variety of receptors inhibitors has been proposed for PDAC, which halts the cross-talk between cancer cells and cancer fibroblast (stromal cells) [7]. Although GEM is a water-soluble

compound, non-specific toxicity and acute hydrophobicity of the adjuvant (such as GDC 0449) often render such combinations challenging for clinical applications. Drug accumulation in specific micro-environmental and intracellular compartments at maximum therapeutic and sub-toxic concentration is also an unmet challenge for this combination delivered using conventional dosage forms [8]. In addition, a high volume of distribution (V_d), fast metabolic clearance rate, frequent dosage administration regimen, drug-associated side effects, and tumor heterogeneity severely reduce the therapeutic gain of the individual drug in the pancreatic cancer setting [9].

Drug delivery methods using nanoparticles have been a well-established approach to improve drug efficacy, enhanced circulation lifetime, and tolerability [10]. While the nanocarrier-assisted drug delivery provides an option to target diseased tissues using small molecular ligands and peptides, extensive investigation has also been conducted designing carrier systems that respond to cancer microenvironment-specific cues such as pH [11–14], hypoxia [15–18], enzyme over-expression [4,19], angiogenesis [20], and signaling pathways regulating apoptosis [21]. Since there is a sharp pH-gradient between stromal to intracellular regions within PDAC micro-environment [22], we hypothesize that a set of nanoparticles composed of amine-rich block copolymers of varying pK$_a$ will be an effective platform to deliver a combination of drugs, where one of the agents could be highly hydrophobic, in a pH-specific pattern. Such condition-specific delivery will be critical to interfere with the growth of and metabolic interactions between cancer cells that drive PDAC growth. The general concept of such spatio-selective activation and synthetic route of such nanoparticle-forming block copolymers is presented in Fig. 1a and b.

An extensive systematic investigation from Hammond et al. has already established the pH-responsive block copolymers of PEG-b-poly (peptide) with tertiary amines as pH-responsive triggers to be an excellent platform for intracellular compartment-specific delivery of cytotoxic agents such as doxorubicin for triple negative breast cancer and ovarian cancer [23–25]. Kataoka et al. [26] and Lecommandoux et al. [27] have shown the efficacy of block copolymers to encapsulate and release both hydrophilic and hydrophobic class of drugs to prostate, breast, and liver cancer cells, and the diversity of tertiary amines as pH-responsive triggers. Mahato et al. [28] recently shown that PEG-b-polycarbonate block copolymer micelles containing conjugated and encapsulated synergistic combination showed enhanced performance in slowing PDAC progression in mice model. Since the appearance of the first report by Hedrick's et al. [29] on PEG-b-poly (carbonate) block copolymer derived from cesium fluoride mediated ring-opening polymerization of pentafluorophenol protected bis (methyl propionic acid), the use and modification of such approach by other groups for drug delivery applications have been reported by Chilkoti et al [30]. Gao et al. have synthesized pH-activable micellar nanoparticles composed of ionizable block copolymers where ionization the of tertiary amines appended to the hydrophobic block resulted in pH-dependent fluorescent readout [31–33]. We envisioned that combining and harnessing the enhanced hydrophobic interactions of the polycarbonate domains of PEG-b-poly (carbonate) block copolymers and pH-specific protonation capacity of tertiary amines to generate a systematically stable, spatio-temporally controlled drug nanocarrier can induce enhanced and targeted accumulation of therapeutic agents to PDAC microenvironment. [6,33,34,1]. To establish the proof-of-concept, we have used a combination of GEM and GDC 0449 (a transmembrane SMO protein inhibitor), which has been proposed to suppress the autocrine and paracrine signalling between cancer cells and stromal cells. Our working hypothesis was that, if we encapsulate GDC-0449 and GEM within PEG-PY and PEG-DB polymersomes and mix these two types of nanoparticles at different stoichiometric ratio, we will obtain spatially controlled release of both the drugs, where the kinetics of release of the individual drug will depend on the mixing ratio of the respective nanoparticles. We also hypothesize that these payloads will be co-released as a function of pH as the nanoparticle population progresses from pH

mimicking desmoplastic, acidified micro-environment (pH 6.9 – 6.5) [35–37] to intracellular pH of acidic compartments such as endosomal-lysosomal pathways (pH 5.5–4.5). We have selected pancreatic cancer to demonstrate the therapeutic efficacy of the proposed system because overexpression of Sonic type Hedgehog receptors is observed in both pre-invasive and invasive epithelium of 70% of human pancreatic cancers, and is absent in normal pancreas irrespective of the progression stage of the disease [38]. In addition, aberrant Hedgehog ligand expression has been found to have a direct association with oncogenic KRAS mutation, which is found in > 95% cases of pancreatic ductal adenocarcinomas (PDAC) [39].

Hence, in this report we report the synthesis and fabrication of a set of pH-responsive nanoparticle constructs that are designed to respond to such dynamically changing pH-environment of PDAC where Hedgehog inhibition is necessary, assess their physicochemical and pH-responsive properties, estimate encapsulation and release of combination agents in response to varying pH, and evaluate interactions with pancreatic cancer cells in *in vitro* and *in vivo* model.

2. Experimental section

2.1. Materials

All chemicals were obtained from Sigma-Aldrich and anhydrous solvents from VWR, EMD Millipore. ^{1}H NMR Spectra were recorded using a Bruker 400 MHz spectrometer using TMS as the internal standard. IR Spectra were recorded using an ATR diamond tip on a Thermo Scientific Nicolet 8700 FTIR instrument. Gel permeation chromatographic measurements were done on a GPC system (EcoSEC HLC-8320GPC, Tosoh Bioscience, Japan) using a differential RI detector, employing polystyrene (Agilent EasiVial PS-H 4 ml) as the standard and THF as the eluent with a flow rate of 0.35 mL per minute at 40 °C. The sample concentration used was 1 mg/mL of which 20 µL was injected. DLS measurements were carried out using a Malvern instrument (Malvern ZS 90). UV–vis and fluorescence spectra were recorded using a Varian UV–vis spectrophotometer and a Fluoro-Log3 fluorescence spectrophotometer respectively. TEM studies were carried out using a JEOL JEM-2100 LaB$_6$ transmission electron microscope (JEOL USA, Peabody, Massachusetts) with an accelerating voltage of 200 kV.

2.2. Synthesis of polymers

PEG-b-poly (carbonates) were synthesized using a macroinitiator, such as poly (ethylene glycol) (PEG, M_n = 5000 g/mol) (1) through a ring opening polymerization of pentafluorophenol protected bis (methoxy propionic acid) derivative 2, according to the synthetic procedures described by Hendricks et al, and later modified by Chilkoti [30] (Fig. 1). The resulting macromolecular intermediate 3 was post-functionalized [40] stoichiometrically using two different amines, namely N, N′dibutylethylenediamine (pK$_a$ = 4.0), and 2-pyrrolidin-1-yl-ethyl-amine (pk$_a$ = 5.4) to synthesize the pH-responsive block copolymers namely PEG-DB (4) [PEG-b-poly(carbonate) appended with *N*, *N*′dibutylethylenediamine side chains] and PEG-PY (5) [*i.e.* PEG-b-poly(carbonate) appended with 2-pyrrolidin-1-yl-ethylamine side chains] respectively. ^{1}H NMR and IR spectroscopy have been carried out to characterize resulting block copolymers and their precursors (Figs. S1–S5, Supporting information). Both 4 and 5 were water soluble at room temperature.

2.3. pK$_a$ determination

Acid dissociation constant, *i.e.*, pK$_a$ values of both copolymers were determined by titrating the aqueous solution of these polymers against 0.1 N sodium hydroxide, and the corresponding monomers were also titrated using the same method. The pK$_a$ was calculated by measuring the pH at the half-equivalence (inflection) point of the titration curve.
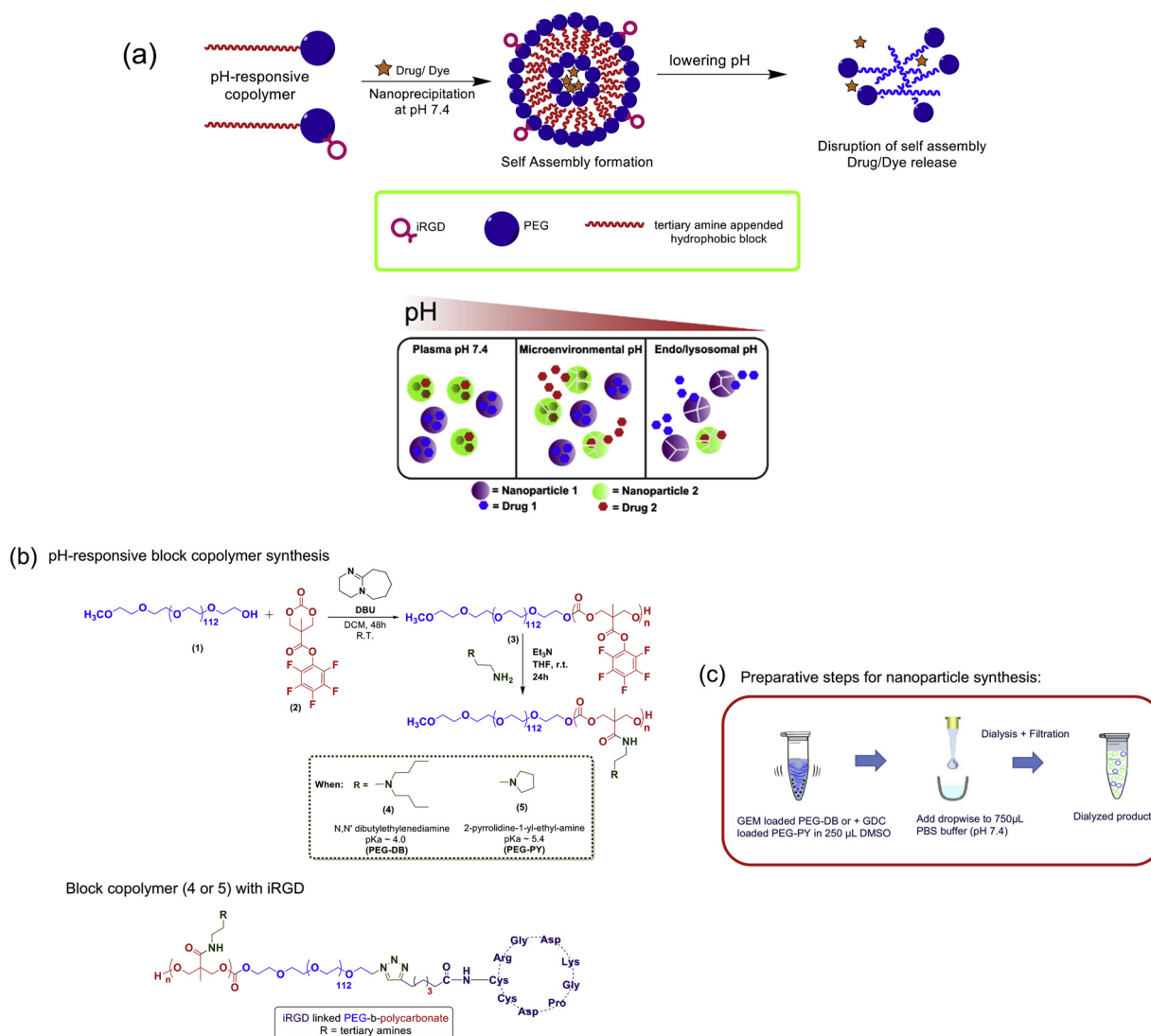
Fig. 1. (a) Mechanism of self-assembly of pH responsive polymers (top panel) and mixed nanoparticle platform for pH-selective drug release (bottom panel). **(b)** Synthetic route to pH-responsive PEG-b-poly (carbonate) copolymer and their iRGD conjugated variant. **(c)** Preparative steps for nanoparticle formulation by nanoprecipitation method.

2.4. Determination of the Critical aggregation constant (CAC) of the polymers

From a stock solution of 0.1 mM pyrene in dichloromethane, 10 μL aliquot was taken in different vials, and the dichloromethane was allowed to dry. To each of these vials, various measured amounts of two different amines substituted polymers was added (stock solution concentration 1 mM) so that the concentrations varied from 0.0019 mM to 0.5 mM and the final concentration of pyrene in each vial was 1 μM. The vials were sonicated for 45 min and then allowed to stand for 3 h before recording the fluorescence spectra [41]. The fluorescence emission spectra were recorded at an excitation wavelength of 337 nm with a bandwidth of 2.5 nm (for both excitation and emission). The ratio of the intensities at 373 nm and 384 nm were plotted against the concentration of the polymer, and the inflection point of the curve was used to determine the CAC.

2.5. Preparation of nanoparticles

To construct the self-assembled structures of amphiphilic block copolymers PEG-DB (**4**) and PEG-PY (**5**) in the form of nanoparticles, the nanoprecipitation method from a selective solvent (DMSO) to a non-

selective solvent (buffer) was employed. To form nanoparticles, 10 mg of PEG-DB (**4**) or PEG-PY (**5**) block copolymers were dissolved in 250 μL of DMSO, and the solution was added drop-wise to 750 μL of PBS buffer (pH 7.4). The resultant solution was transferred to a float-a-lyzer (MWCO 3.5–5 kDa) and allowed to dialyze against ∼ 700 mL PBS buffer (pH 7.4) overnight with constant shaking at moderate speed. The solutions were then filtered using a 0.2 μm PES filter and the size measured using DLS (Dynamic Light Scattering) studies at a scattering angle of 90°.

2.6. Formation of targeted nanoparticles: synthesis of iRGD containing (4) and (5)

To synthesize the peptide containing polymersomes, iRGD hexanoic acid was "clicked" with azide-(**4**) and azide-(**5**) separately. Briefly, azide-containing **4** and **5** and the peptide were separately dissolved in deionized water (5 mg/mL, for the peptide, using sonication in iced water). For 5 mg of polymer 16 μL of Cu-ascorbate complex and 16 μL of the sodium ascorbate (27 mg/mL in deionized water) was added and the reaction was allowed to stir at room temperature for 24 h. Following the reaction, the contents were moved to a dialysis bag (MWCO 1000 Da) and dialyzed for 72 h with a media change every

24 h. The contents of the dialysis bag were subsequently lyophilized and analyzed. A 1-mg/mL aqueous solution of the freeze-dried product and the polymer prior to conjugation with the peptide were analyzed using CD spectroscopy.

2.7. Encapsulation and release of carboxyfluorescein from pH-responsive nanoparticles

Following the protocol described by Mallik et al. [18], 5(6)-carboxyfluorescein (CF) encapsulation was carried out by preparing a stock solution of 1 mM carboxyfluorescein in PBS buffer (137 mM NaCl, pH 7.4) and adding 250 μL of the polymers (10 mg/ mL) to 2 mL of the dye solution in a drop-wise pattern with constant stirring. The resulting solution was allowed to stir for an hour followed by sonication for 60 min and dialyzed overnight using a float-a-lyzer (MWCO 3.5–5 k Da) against 700 mL PBS buffer. The media was changed completely to maintain sink condition, and dialysis was continued for another 6 h until no further discoloration of the media was observed. The release of carboxyfluorescein from polymersomes was studied at different pH (4.5 and 7.4 for PEG-DB polymersomes and pH 5.5 and pH 7.4 for PEG-PY polymersomes) by measuring the fluorescence emission intensity by exciting the respective release solutions at 492 nm and recording the emission intensities at 515 nm (Supporting information, Fig. S7). After 5 h, 20 μL of Triton was added to disintegrate the polymersomes and the fluorescence emission intensity measured for total release after disintegration. Percentage release was calculated using the formula, and the cumulative percentage release was plotted against time:

$$
\% \, release
$$
$$
= \frac{Emission \, intensity \, after \, release \, - \, Emission \, intensity \, before \, release}{Intensity \, after \, Triton \, treatment \, - \, Emission \, intensity \, before \, release}
$$
$$
\times \, 100
$$

2.8. Encapsulation of drug(s) and dye in block copolymeric nanoparticles

For preparation of drug loaded copolymeric nanoparticles, 10 mg of the respective block copolymer were dissolved in 250 μL of DMSO in the presence of 5 mg of drugs (either GEM or GDC). The solution was added dropwise to a stirring solution of 750 μL of PBS buffer. The solution was allowed to stir for overnight followed by centrifugation using micro-centrifuge filters at 500 rpm. The filtrate was analyzed using UV–vis spectroscopy for quantification of the amount of drug loaded within nanoparticles. For dye (such as Alexa Fluor 647 encapsulation, 10 mg of the polymer and 50 μL of the dye were dissolved in 250 μL of DMSO. The solution was added to a 750 μL solution of PBS under vigorous stirring in a dropwise pattern. The solution was stirred for an hour, and dialyzed using a float-a-lyzer of MWCO of 3.5–5 kDa against 800 mL of buffer.

2.9. In vitro drug release experiments

Drug release experiment was conducted by taking 1 mL of the drug-loaded nanoparticle solution in a float-a-lyzer (MWCO 3.5–5 kDa). Nanoparticle solution was composed of GEM loaded PEG-DB, and GDC loaded PEG-PY polymersomes mixed at 1:1, 1:4, and 4:1 ratio respectively. The respective solution was immersed in 5 mL of buffer maintained at a desired pH. A specified volume of the bulk solution was withdrawn periodically and replaced by equal volume of fresh buffer of similar pH to maintain the sink condition. Dye release experiment was conducted analogously for a fixed ratio.

2.10. In vitro cell culture

The pancreatic cancer cell line, BxPC-3 and Mia PaCa-2 were from American Type Culture Collection and grown at 37 °C with 5% CO_2. The BxPC-3 cells were cultured in RPMI media (Hyclone) supplemented with 10% fetal bovine serum (Hyclone) and 1% penicillin/streptomycin (Corning). MiaPaCa-2 cells were cultured in DMEM high glucose medium (Thermo Fisher Scientific) supplemented with 10% fetal bovine serum and 2.5% horse serum (Corning). The cell lines were subcultured by enzymatic digestion with 0.25% trypsin/ 1 mM EDTA solution (Thermo Fisher Scientific) when they reached approximately 70% confluency.

2.11. Cell viability assay

Cytotoxicity of PEG-DB and PEG-PY either as unassembled block copolymers or encapsulated with GEM and GDC 0449 were tested on both BxPC-3 and MiaPaCa-2 cells. For BxPC-3 cells, 5000 cells/well were plated. After 24 h, the cells were treated with 0.8 μM of GEM encapsulated PEG-PY and 1.5 μM GDC encapsulated PEG-DB nanoparticles. For MiaPaCa-2, 1000 cells/well were seeded in 96-well plates and 24 h later, were treated with different concentration of PEG-DB, PEG-PY block copolymers or drug-encapsulated nanoparticles from at different concentrations. For this cell line, the concentration of free or nanoparticle encapsulated GDC was kept constant at 10 nM, and the concentration of GEM (free or encapsulated) were varied from 0 to 100 nM. After 72 h incubation, cell viability assay was performed by MTS assay.

2.12. Cellular uptake studies

MiaPaCa-2 cells were plated in 6-well plates at 5000 cells/well and were allowed to grow to 70% confluence. The cells were then incubated overnight with either targeted or non-targeted fluorescently (Alexa Fluor 647) labeled nanoparticles (at a concentration of 0.5 mg/mL) at 37 °C. After the incubation period, the cells were washed with cold PBS (3X), trypsinized, and resuspended in PBS. Propidium iodide (PI) staining was used to identify the live and the dead cell population. Subsequently, the cells were suspended in a flow cytometry buffer (PBS with 0.1% BSA), and the cell-associated fluorescence intensity of Alexa Fluor 647 was determined by BD Biosciences Accuri C6 Flow Cytometer. Three technical replicates were included for each experiment, and the experiments were performed in biological triplicates.

2.13. Confocal microscopy

Cellular uptake of nanoparticles constituted from PEG-b-poly (carbonate) block copolymers was assessed by confocal fluorescence microscopy. The confocal images were taken using Zeiss AxioObserver Z1 microscope equipped with LSM700 laser scanning module (Zeiss, Thornwood, NY), at 40X magnification with40x/1.3 Plan-Apochromat lens. MiaPaCa-2 cells were seeded in ibidi® glass bottom dish (35 mm) at 1×10^5 cells per well and grown overnight. Then, cells were incubated with polymersome at 37 °C in DMEM high glucose medium for 24 h. At the end of this period, cells were washed with PBS and followed by addition of Opti-MEM and imaging.

2.14. In vivo experiments

Xenografts were established by injecting 0.1 mL of 8×10^7 BxPC-3 Cells without Matrigel® basement membrane matrix on the hind flank of six- to eight week old athymic nude mice (Nu/Nu). Before establishing the xenograft, the mice were maintained in sterile conditions using the Innovive IVC system (Innovive), following a protocol approved by North Dakota State University's Institutional Animal Care and Use Committee. An acclimatization period of 1 week has been allowed before experimental manipulation. Tumors were allowed to form for 3 weeks. Fluorescently-tagged nanocarrier suspension (100 μL, 10 mg/mL equivalent concentration of PEG-DB containing 5% iRGD-bound PEG-DB) were injected *via* the tail vein, and the tumors were harvested after

24 h and processed by Advanced Imaging and Microscopy Laboratory at NDSU. Briefly, tumor tissues from control and nanoparticle-treated mice were collected and fixed for 24 h in formaldehyde. Paraffin-embedded 5 μm thick sections of tumor tissues were deparaffinized with Histo-Clear and ethanol, followed by antigen retrieval in 10 mM sodium citrate buffer (0.05% Tween 20, pH 6.0) using an autoclave method. The sections were blocked for 20 min using blocking buffer (10% normal goat serum in TBST) and incubated with S100 (Abcam, UK) primary antibody for 1 h at room temperature followed by FITC-labeled secondary antibody (Biotium, Fremont, CA). After mounting a coverslip using Hardset Mounting Medium with DAPI (Vector Labs, Burlingame, CA), slides were visualized using a Zeiss AxioObserver Z1 confocal microscope (Zeiss, Thornwood, NY).

3. Results and discussion

3.1. Self-assembly and aggregation properties of pH-responsive block copolymers

Block copolymers form a stable nanoparticle assembly as micelles or polymersomes where hydrophobic and hydrophilic blocks assist the formation of such structures [10,33,42]. These nanoparticles can encapsulate a wide variety of small molecular weight compounds such as drugs and dyes [27]. We synthesized PEG-b-poly (carbonates) block copolymers and used two different tertiary amine groups attached to the hydrophobic blocks to regulate their pK_a values. In addition, we have also immobilized the iRGD peptide (a cyclic oligopeptide that can recognize neuropilin and integrin receptors) onto the PEG block of these copolymers to augment cellular uptake. The synthetic scheme of the block copolymers is presented in Fig. 1b. First, we determined the pK_a values of the block architectures and compared with that of the corresponding monomers. Fig. 2a shows the titration curves of 4 and 5,

indicating the net pK_a values were at 5.53 ± 0.14 and 6.83 ± 0.23 (n = 2) respectively. The pK_a was estimated by measuring the pH at the half-equivalence (inflection) point of the titration curve. These values indicated that, at these mildly acidic pHs, at least 50% of PEG-DB and PEG-PY block copolymers would remain in ionized (protonated) form facilitating the amphiphilic to hydrophilic transition, which will result in destabilization of their self-assembled structures that would otherwise be stable at plasma pH of 7.4. Hence, the destabilization pH of these copolymeric block self-assemblies can be harnessed to initiate drug release at desmoplastic and intracellular pH. PEG-PY nanoparticles, composed of the block copolymer (5) were found to have an average hydrodynamic diameter in the range of 117 ± 9.8 nm, while PEG-DB derived nanoparticles (constructed from block copolymer 4) showed an average diameter of 149 ± 14.4 nm (Fig. 2b). TEM studies also showed the presence of spherical particles although a fraction of smaller particles (Fig. 2c and d) was observed which also correlates with dynamic light scattering data as shown in Fig. 2b [43]. The difference between the sizes of PEG-PY and PEG-DB nanoparticles can be attributed to the molecular structures of the side chains appended to the hydrophobic blocks of the nanoparticle-forming block copolymers. While PEG-PY block copolymers are appended with a strained cyclobutyl amine side chain at their hydrophobic polycarbonate block, PEG-DB systems contain the aliphatic n-butyl amines at the similar domain, likely resulting in nanoparticles larger in size than their PEG-PY counterpart. Following Eisenberg's [42,44] earlier work, since the ratio of the mass of the hydrophobic block to the total polymer mass (known as the f value) for both 4 and 5 lies typically between 0.35 and 0.45, the resulting PE-PY and PEG-DB nanoparticles are most likely to have polymersome-like architectures. However, in TEM image we did not observe any bilayer structure, rather a solid colloidal nanoparticles were found with an average diameter of 50–80 nm, most likely due to shrinkage of the nanoparticles upon drying (Fig. 2c and d and
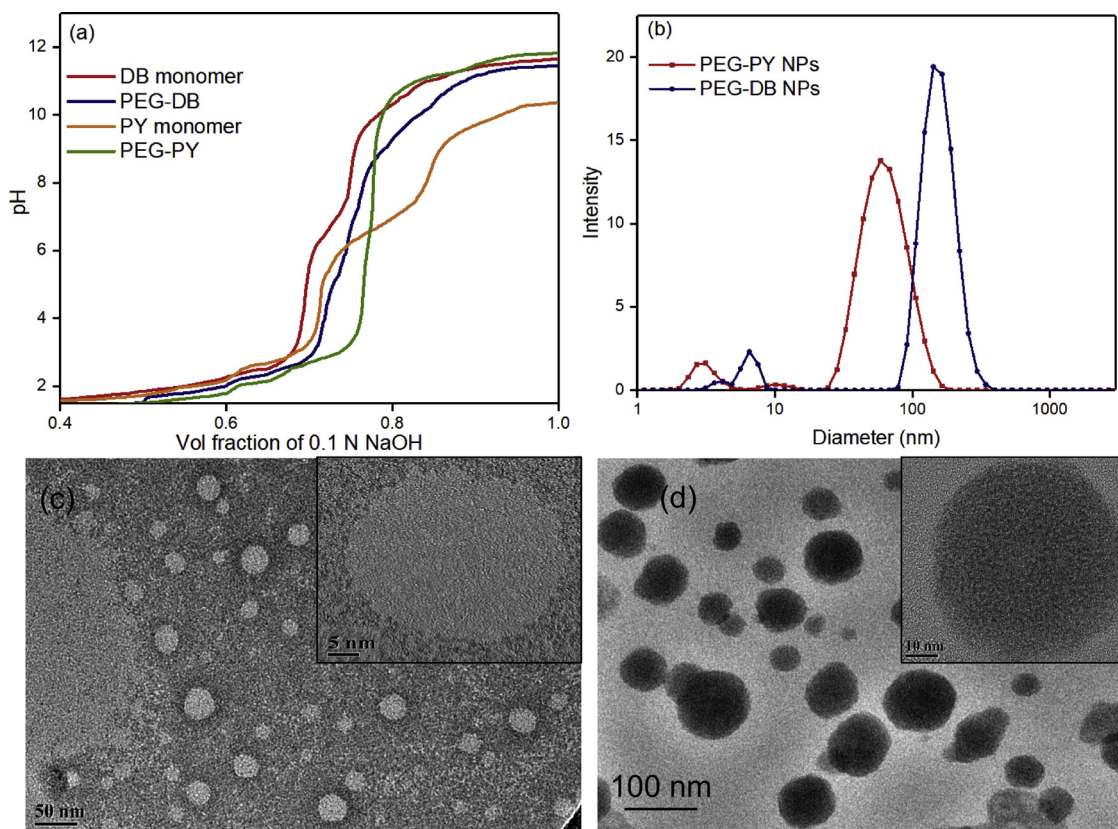

Fig. 2. (a) pH titration curves of the block copolymers and their corresponding monomers (b) Size distribution of nanoparticles by DLS (c) TEM of PEG-PY (5) NPs and HRTEM of a single nanoparticle (inset) (d) TEM image of PEG-DB (4) NPs and HRTEM of a single PEG-DB nanoparticle (inset).
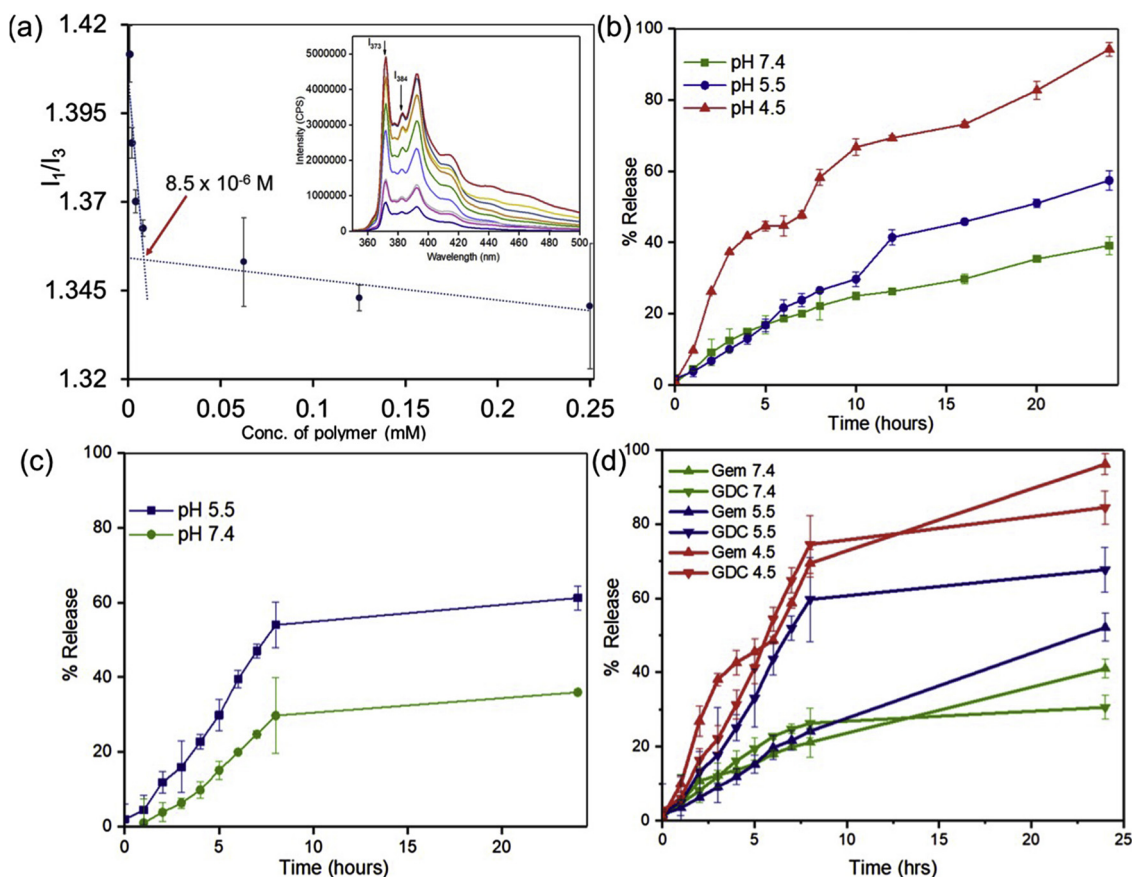
Fig. 3. (**a**) Plot of I_1/I_3 of 10^{-6} M of pyrene encapsulated in varying concentrations of PEG-DB (**4**). Fluorescence emission spectra of pyrene in the presence of PEG-DB (λ_{ex} = 337 nm) are shown in the inset. Corresponding error bars represent standard deviations n = 3. (**b**) Cumulative percent release of Gemcitabine from PEG-DB polymersomes at pH 4.5, 5.5, and 7.4 (**c**) Corresponding release profile for GDC 0449 encapsulated in PEG-PY polymersomes at pH 5.5 and pH 7.4 Error bars represent standard deviations when n = 3. (**d**) Cumulative percentage release of GEM and GDC from 1:1 v/v mixture of drug-encapsulated PEG-DB and PEG-PY nanoparticles at different pH environment. Error bars represent standard deviation of the average of three measurements (n = 3).

Supporting information, Fig. S6. Immobilization of the iRGD peptide onto nanoparticle surface was not found to alter the particle size or distribution significantly (Supporting information, Fig. S7).

3.2. Determination of critical association concentration (CAC) of block copolymers

The aggregation properties of the block copolymer **4** and **5** were then evaluated at pH 7.4 using pyrene as the probe [41]. It has been reported that the first (λ_{373} nm) and third (λ_{384} nm) peaks in the fluorescence emission spectra of pyrene are sensitive to the polarity of the environment and, the ratio of these two signals can be used to determine the stability of association of block copolymers as micelles or polymersomes [45]. We observed that the ratio of I_{373}/I_{384} gradually decreased as the polymer concentration was increased up to a concentration of 8.5 μM for **4** (Fig. 3a) and 20 μM for **5** (Supporting information, Fig. S8), after which the I_{373}/I_{384} ratio remained mostly unchanged. The value of I_1/I_3 at the breakpoint (1.35, Fig. 3a for **4**) leads to the inference that the probe is located in a hydrophobic environment created by the aggregation of the hydrophobic segments beyond the critical association concentration of the respective block copolymers. The critical aggregation concentration (CAC) values obtained for **4,** and **5** were in the order of 8.5×10^{-6} and 2.0×10^{-5} M respectively and found to be comparable to polyesters and polypeptide-derived block copolymers [46]. The CAC value for copolymer **5** is presented in Supporting information, Fig. S8b. Lower CAC values with **4** can be attributed to butyl chains of the tertiary amine which likely to form stronger hydrophobic entanglement than their cycloaliphatic

counterpart **5**. This experiment established that both **4** and **5** lead to the formation of PEG-DB and PEG-PY nanoparticles, which are sufficiently stable at pH 7.4 usable for systemic administration.

3.3. pH-dependent disassembly and content release from nanoparticles

This is to note that, GEM (log P = −1.4), is a frontline chemotherapeutic agent for pancreatic cancer, which inhibits DNA repair and replication [47], while GDC 0449 (vismodegib, log P = 2.7) is a potent systemic inhibitor of Hh signal transduction [48] mediated by inhibition of transmembrane SMO proteins [49]. Both the drugs presented widely different lipophilicities to encapsulate in a conventional polymeric, such as poly (lactic acid-co-glycolic acid) or lipid-based nanoparticles. To establish the mechanistic stability and the pH-responsive properties of nanoparticles at microenvironmental and intracellular pH-range, we first encapsulated a self-quenching hydrophobic dye 5(6)-carboxyfluorescein (CF) within PEG-DB and PEG-PY nanoparticles. We investigated the kinetics of the released CF as a function of time by measuring its fluorescence intensity in aqueous media [18]. For CF encapsulated in PEG-DB nanoparticles, the release was studied at both pH 4.5 and 7.4, while pH 5.5 and 7.4 were selected for investigating the release profile of CF from PEG-PY systems (Supporting information, Fig. S9). It was observed that, for PEG-DB systems, almost 100% of the dye was released by 7 h at pH 4.5 (mimicking late-endosomal/lysosomal pH) while only 5% release at pH 7.4 (Supporting information, Fig. S9a). In case of PEG-PY NPs, about 80% of CF was released at pH 5.5 (mimicking PDAC microenvironmental pH) the end of 5 h compared to 18% of content that released over the same

timeframe at pH 7.4 (Supporting information, Fig. S9b). This indicates the stability of the polymersomes at pH 7.4 and their eventual protonation and destabilization of the self-assembled structures promoting compartment-specific, pH-dependent drug release. Following the release behavior of carboxyfluorescein, we set out to encapsulate GEM within PEG-DB nanoparticles, and GDC 0449 within PEG-PY systems. For PEG-DB nanoparticles, encapsulation efficiency of GEM was found to be 86 ± 3.18%, and the loading content was calculated as 29 ± 7.5%, using the equation as described in the supporting information (for n = 5 separate analysis).   The high loading content and efficiency of GEM is most likely attributed to the multiple dibutylamine groups in the hydrophobic block of the copolymer. On the other hand, for PEG-PY system, the loading content and efficiency for GDC was found to be 13 ± 2.9% and 26 ± 3.5%, respectively (n = 5 separate analysis). The release of the encapsulated drugs from nanoparticles was monitored for 24 h at regular intervals in different pH conditions (Fig. 3b and c). While for PEG-DB nanoparticles, the cumulative percentage release of gemcitabine was found to be about 100% at the end of 24 h at pH 4.5, only 38% release was observed at pH 7.4 (Fig. 3b). When tested at pH 5.5, the extent of cumulative release of the drug was greater than that from pH 7.4 but substantially lower than that in pH 4.5 (Fig. 3b). On the other hand for GDC 0449 encapsulated PEG-PY nanoparticles, ~62% and 35% of GDC 0449 was released at pH 5.5 and pH 7.4 respectively at the end of 24 h (Fig. 3c). The differential release of GEM at pH 4.5 and 5.5 from PEG-DB systems indicate the capacity of these nanoparticles to ensure maximum concentration of GEM to be released intracellularly rather in extracellular space. On the other hand, PEG-PY systems will trigger most of the payload release at the microenvironment mimicking pH of 5.5 thus promoting accumulation of the drug in the extracellular space. Although at current degree of functionalization of the pH-responsive side chains, we do observe ~35% of drug release at pH 7.4, most likely by optimizing the length of the hydrophobic block and PEG molecular weight, such non-specific release of GDC 0449 could be suppressed. This is to note that, release experiment for GDC loaded PEG-PY system was conducted only at pH 5.5 and not in lower pH conditions, as the release of this agent is expected to happen in extracellular compartments.

To evaluate the extent of release for GEM and GDC as a function of pH and time from mixed nanoparticle platform, we have incubated a 1:1 mixture (v/v) of PEG-DB (containing GEM) and PEG-PY (containing GDC) nanoparticle in a buffered solution of pH 7.4, 5.5 and 4.5 (Fig. 3d). We observed that, at pH 7.4, the release of GEM and GDC were below 40% of the encapsulated dose over 24 h. At lower pH of 5.5, GEM release was significantly sustained from PEG-DB nanoparticles than that of GDC from PEG-PY particles (52% of encapsulated GDC was released after 8 h, compared to 20% of GEM released over the same period, Fig. 3d). Further lowering of pH to 4.5, did not enhance the release of GDC significantly from PEG-PY system, but led to an approximately 3-fold increase of GEM release from PEG-DB system. Complete protonation of PEG-DB at pH 4.5 and partial protonation of the same at pH 5.5 is most likely to be the governing factor for such differential release in case of GEM from PEG-DB block copolymer assemblies. To provide the proof-of-concept of how the gradual decrease of pH from the blood to the endosomal-lysosomal compartment would affect the release of encapsulated materials from synthesized nanoparticles, we investigated the release of a model dye, Alexa Fluor 647 encapsulated within PEG-DB nanoparticles in gradually changing pH conditions (Fig. S10, Supporting information). First, the nanoparticle solution was incubated in pH 7.4, and the pH of the release medium was gradually reduced after every 3 h by the addition of 0.1 N HCl. We observed that less than 10% of the encapsulated dye was released at pH 7.4 for the first 3 h from PEG-DB nanoparticles. At pH 5.5, which mimics the pH of extracellular space, approximately 2-fold enhancement of cumulative release of the dye from PEG-DB nanoparticles. Finally, when the pH was further lowered to intracellular pH (mimicking late endosomal-lysosomal pH), the release of Alexa Fluor 647 from the

nanoparticle system was significantly enhanced after a period of 6 h (Fig. 3d) indicating an almost quantitative pH-activated release of the encapsulated content from PEG-DB block copolymeric nanoparticles. After investigating the release kinetics of individual drugs from respective nanoparticles mixed at 1:1 ratio, we set out to investigate the effect of pH-mediated release when the mixture has a different ratio of nanoparticles other than 1:1. It is interesting to note that, when we changed the ratio of the two nanoparticles from 1:1 of to 1:4 or 4:1 (PEG-DB: PEG-PY nanoparticles respectively), we did not observe any significant change of release at pH 7.4. This observation indicates that the nanoparticles will remain intact in systemic circulation independent of mixing ratio (Fig. S11, Supporting information). At pH 4.5, we observed the faster release of GEM after 8 h, likely due to increased protonation of GEM overcompensating the effect of mixing-ratio of nanoparticles. More prominent effect of mixing ratio was observed at pH 5.5 (blue lines, Fig. S11, Supporting information), where the difference of release between the two drugs after 8 h was reduced by 2 (for 4:1 of PEG-DB to PEG-PY) to 8-fold (for 1:4 of PEG-DB to PEG-PY) than that obtained when the nanoparticle population was mixed at 1:1 ratio. This experiment indicates that for a nanoparticle-delivered combination therapy, it is be possible to change kinetics and availability of individual drug at a particular target by altering the ratio of the nanoparticles.

3.4. In vitro cytotoxicity of pH-responsive nanoparticles

We have then evaluated the cellular compatibility of the block copolymers and *in vitro* performance of drug-loaded PEG-DB and PEG-PY nanoparticles to suppress growth and proliferation of two pancreatic cancer cell lines, such as BxPC-3 and Mia PaCa-2. We set out to show the efficiency of the synthesized nanoparticles in these two types of cell lines, such as Mia PaCa-2, which shows KRAS mutation, and BxPC-3 which contains wild-type RAS and are not RAS activated [50]. This is to note that, KRAS mutation is more prevalent in human pancreatic cancer. In addition, these two cell lines also show different metabolic activity. Mia PaCa-2 is strongly glycolytic, while BxPC-3 is mildly glycolytic, and this is well postulated that chemotherapeutic success critically depends on the metabolic profiling of target cancer cells [51]. First, we evaluated the viability of Mia PaCa-2 cells when treated with PEG-DB and PEG-Py block copolymers without the drug, to assess the inherent cytotoxicity of nanoparticles alone (Fig. 4a). We have also studied the viability of fibroblast cells when treated with drug-free nanoparticles as well as with the structural components of the particle-forming block copolymers separately, such as, PEG (the hydrophilic block of the copolymer), poly (carbonate) block appended with *N*, *N'*-dibutyl ethylenediamine (PC-DB, the hydrophobic block of the copolymer) and *N*, *N'*-dibutyl ethylenediamine (DB) alone (Fig. S12, Supporting information). For therapeutic efficiency study, the cells were treated with single or combination therapy of GEM and GDC 0449, either alone or encapsulated within PEG-DB nanoparticles (Fig. 4b and c). Fig. 4a reveals that after 48 h of treatment, block copolymers PEG-DB (**4**) and PEG-PY (**5**), in their unassembled form, are non-toxic to Mia PaCa-2 cells within a concentration range of 1.25 to 0.2 mg/mL. Fig. 4b shows that GEM encapsulated within PEG-DB at a concentration of 0.8 μM is more effective when combined with PEG-PY encapsulated GDC (1.5 μM) than the combination of free drugs in BxPC-3 cell lines in a similar concentration. We also observed that, when Mia PaCa-2 cells were treated with increasing concentration of GEM in the presence of 10 nM of GDC (either free or encapsulated within PEG-PY system), nanoparticle bound formulations brought in enhanced more cytotoxic onslaught than combination of free drugs (Fig. 4c).

3.5. Cellular and tissue internalization of nanoparticles

To investigate the potential of PEG-b-polycarbonate block copolymers to form nanoparticles with enhanced cellular uptake and tissue
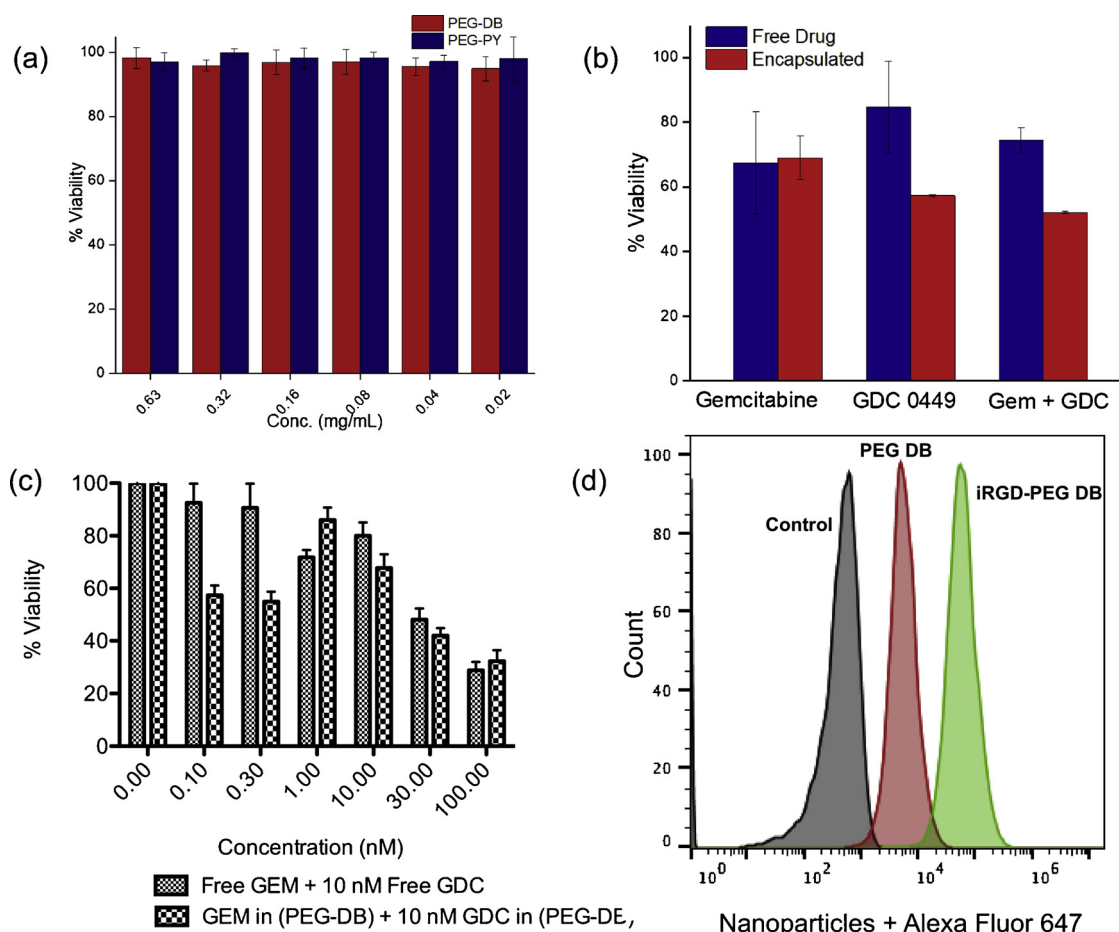
Fig. 4. (a) Both PEG-DB and PEG-PY block copolymers in their unassembled form are non-toxic to MIAPaCa-2 cells (N = 3) (b) Cell viability for GEM (0.8 μM) encapsulated in PEG-DB and GDC 0449 (1.5 μM) in PEG-PY NPs in BxPC-3 cells. (c) Cellular viability studies of Mia PaCa-2 cells when treated with increasing concentration of GEM in either free or PEG-DB encapsulated form in the presence of 10 nM GDC (free or PEG-PY encapsulated form, N = 3) **(d)** Immobilization of iRGD peptide on PEG-DB nanoparticles enhances uptake of the nanoparticles in Mia PaCa-2 cells at 37 °C.

penetration property to use in desmoplastic PDAC tumor, we have immobilized a cyclic peptide, iRGD, onto PEG-DB nanoparticle surface (Fig. 1b, S13, Supporting information). This cyclic peptide has been reported to bind selectively to the integrin ($\alpha_v\beta_5$) and Neuropilin receptors overexpressed in the tumor blood vessels thus enhancing the capabilities of nanoparticles carrying encapsulated materials to penetrate further into the desmoplastic stroma of PDAC microenvironment [52,53]. Polymersomes decorated with iRGD were synthesized by conjugating the peptide to block copolymer (**4**) through Cu^{2+}-catalyzed azide-alkyne click chemistry and characterized using CD (Supporting information, Fig. S13) and IR spectroscopy. Since Mia PaCa-2 cells have been well reported to bear integrin receptors [54], we have conducted Flow cytometry experiments in MIA PaCa-2. Flow cytometry data clearly showed significant uptake of iRGD-decorated PEG-DB nanoparticles compared to untargeted polymersomes, which is a contribution from both non-specific endocytosis and receptor-mediated uptake of targeted nanoparticles (Fig. 4d). Confocal fluorescence microscopy experiment supported the flow cytometric observation in the same cell line, where an augmented cell-associated fluorescence from iRGD-containing PEG-DB nanoparticles labeled with Alexa Fluor 647 was observed within the cytosol of MIAPaCa-2 cells (Fig. 5b) compared to cells treated with non-targeted nanoparticles (Fig. 5a).

To obtain preliminary information on the internalization capacity of pH-responsive nanoparticles within cancer microenvironment *in vivo* in a mouse model, we have grown BxPC-3 tumor xenograft in immune compromised nude mice. Due to the slow growth rate of MiaPaca-2 cells as xenografts; we used BxPC-3 cells, which formed the tumor

xenograft within 3 weeks. We have selected PEG-DB as a representative class of nanoparticles and injected the labeled nanoparticle solution through tail-vein. After 6 h post circulation and necropsy, we observed that i.v. administered, fluorescently tagged PEG-DB nanoparticles accumulating in tumor microenvironment as visualized in the histologic cross-section image of excised tumor tissue in Fig. 5(d). This result is consistent with the notion that most nanoparticles within the size range of 100–150 nm are most likely accumulated into tumor microenvironment by size-dependent, passive targeting mechanism. Tissue targeting can be augmented by immobilizing different targeting ligands, such as iRGD, on nanoparticle surface [55]

4. Conclusions

In this report, we describe the synthesis and efficiency studies of poly (carbonate)-derived amphiphilic block copolymeric assembly with tunable pH-responsivity. We observed that these assemblies form stable nanoparticles that can encapsulate a drug combination applicable to pancreatic cancer. By stoichiometric mixing of nanoparticles formed from different types of pH-responsive amphiphilic block copolymers, it was possible to achieve drug release as a function of pH corresponding to extracellular tumor microenvironment or in intracellular milieu mimicking pH. Tissue targeting by delivery systems is a Currently, we are working on the extensive intracellular and in-vivo investigations of targeted PEG-b-poly (carbonate) pH-responsive platform for PDAC drug delivery applications.
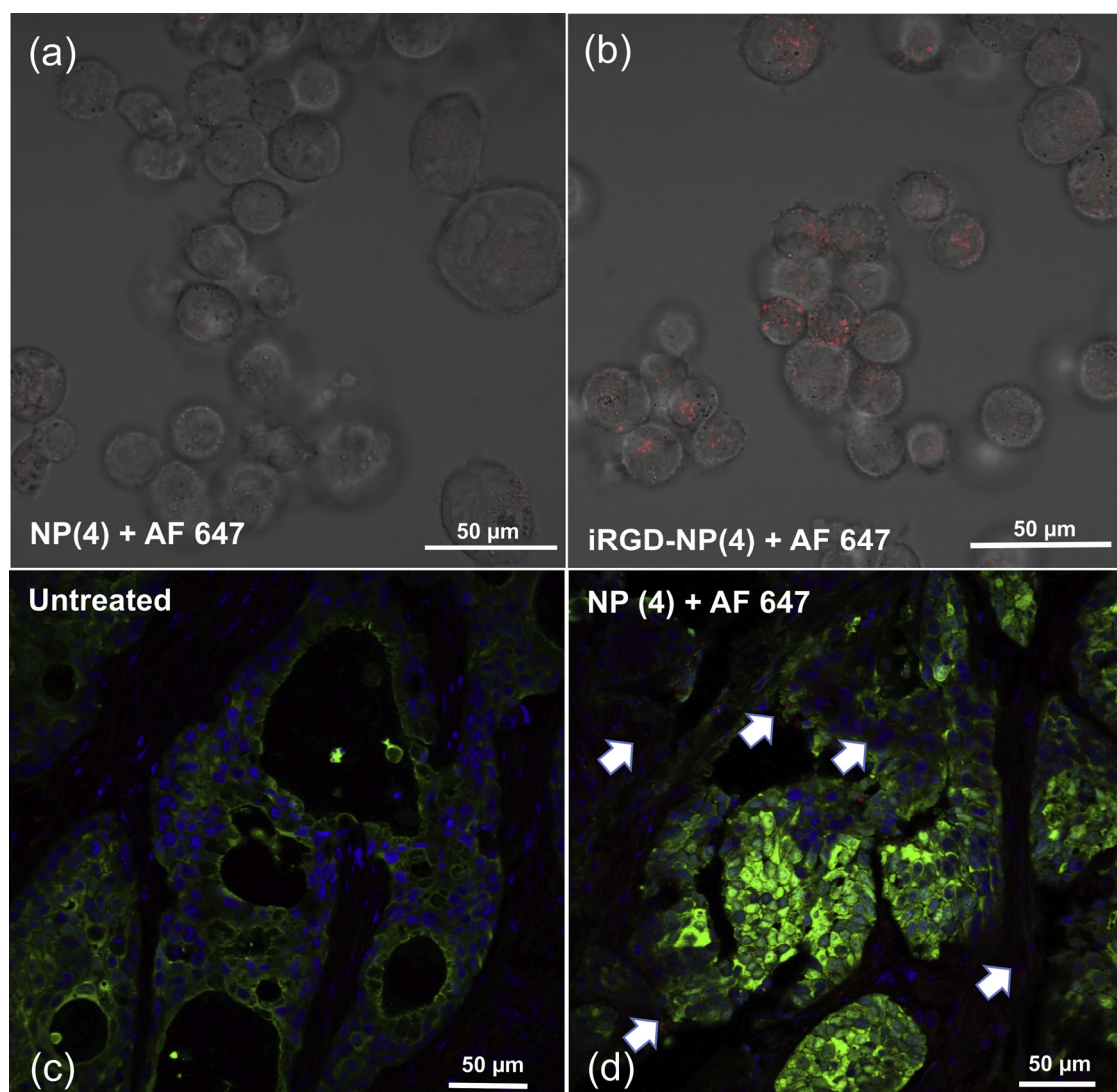
Fig. 5. Top panel: Confocal fluorescence micrograph shows augmented cellular uptake in MiaPaCa-2 cells for iRGD functionalized PEG-DB nanoparticles (**a**) unfunctionalized PEG-DB nanoparticles (**b**) iRGD functionalized PEG-DB nanoparticles. Bottom panel: Histology of tumor section in xenograft bearing mice i.v. injected with PEG-DB AF 647 nanoparticles showing the presence of nanoparticles (red) in (**d**) compared to histology of the tumor section from untreated mice (**c**). Green: FITC labeled S100 positive xenograft cells, Red: Alexa Fluor 647 labelled nanocarrier, Blue: Cell nuclei (For interpretation of the references to colour in this figure legend, the reader is referred to the web version of this article).

Competing financial interest

The authors declare no competing financial interest.

Appendix A. Supplementary data

Supplementary material related to this article can be found, in the online version, at doi:https://doi.org/10.1016/j.colsurfb.2018.10.069.

References

[1] L.E. Gerweck, K. Seetharaman, Cellular pH gradient in tumor versus normal tissue: potential exploitation for the treatment of cancer, Cancer Res. 56 (1996) 1194–1198.
[2] T. Koltai, Cancer: fundamentals behind pH targeting and the double edged approach, Onco. Ther. 9 (2016) 6343–6360.
[3] G.R. Martin, R.K. Jain, Noninvasive measurement of interstitial pH profiles in normal and neoplastic tissue using fluorescence ratio imaging microscopy, Cancer Res. 54 (1994) 5670–5674.
[4] V.P. Chauhan, R.K. Jain, Strategies for advancing cancer nanomedicine, Nat. Mater. 12 (2013) 958–962.
[5] J.M. Bailey, A.M. Mohr, M.A. Hollingsworth, Sonic hedgehog paracrine signaling regulates metastatis and lymphangiogenesis in pancreatic cancer, Oncogene 28

(2010) 3513–3525.

[6] Z. Cruz-Monserrate, C.L. Roland, D. Deng, T. Arumugam, A. Moshnikova, O.A. Andreev, et al., Targeting pancreatic ductal adenocarcinoma acidic microenvironment, Sci. Rep. 4 (2014) 4410.

[7] I. Dickson, Stromal–cancer cell crosstalk supports tumour metabolism, Nat. Rev. Gastroenterol. Hepatol. 13 (2016) 558.

[8] R. Siegel, D. Naishadham, A. Jemal, Cancer statistics, 2012, CA Cancer J. Clin. 62 (2012) 10–29.

[9] E.C. Dreaden, Y.W. Kong, S.W. Morton, S. Correa, K.Y. Choi, K.E. Shopsowitz, et al., Tumor-targeted synergistic blockade of MAPK and PI3K from a layer-by-layer nanoparticle, Clin. Cancer Res. 21 (2015) 4410–4419.

[10] M.E. Davis, Z. Chen, D.M. Shin, Nanoparticle therapeutics: an emerging treatment modality for cancer, Nat. Rev. Drug Discov. 7 (2008) 771–782.

[11] V. Huber, C. Camisaschi, A. Berzi, S. Ferro, L. Lugini, T. Triulzi, et al., Cancer acidity: an ultimate frontier of tumor immune escape and a novel target of immunomodulation, Semin. Cancer Biol. 43 (2017) 74–89.

[12] Y. Kato, S. Ozawa, C. Miyamoto, Y. Maehata, A. Suzuki, T. Maeda, et al., Acidic extracellular microenvironment and cancer, Cancer Cell Int. 13 (2013) 89.

[13] S. Harguindey, S.J. Reshkin, "The new pH-centric anticancer paradigm in oncology and medicine"; SCB, 2017, Semin. Cancer Biol. 43 (2017) 1–4.

[14] S. Granja, D. Tavares-Valente, O. Queirós, F. Baltazar, Value of pH regulators in the diagnosis, prognosis and treatment of cancer, Semin. Cancer Biol. 43 (2017) 17–34.

[15] N. Akakura, M. Kobayashi, I. Horiuchi, A. Suzuki, J. Wang, J. Chen, et al., Constitutive expression of hypoxia-inducible Factor-1α renders pancreatic cancer cells resistant to apoptosis induced by hypoxia and nutrient deprivation, Cancer Res. 61 (2001) 6548–6554.

[16] C. Feig, A. Gopinathan, A. Neesse, D.S. Chan, N. Cook, D.A. Tuveson, The pancreas cancer microenvironment, Clin. Cancer Res. 18 (2012) 4266–4276.

[17] P. Vaupel, A. Mayer, Hypoxia in cancer: significance and impact on clinical outcome, Cancer Metastasis Rev. 26 (2007) 225–239.

[18] P. Kulkarni, M.K. Haldar, S. You, Y. Choi, S. Mallik, Hypoxia-responsive polymersomes for drug delivery to hypoxic pancreatic cancer cells, Biomacromolecules 17 (2016) 2507–2513.

[19] D.J. Shields, S. Niessen, E.A. Murphy, A. Mielgo, J.S. Desgrosellier, S.K. Lau, et al., RBBP9: a tumor-associated serine hydrolase activity required for pancreatic neoplasia, Proc. Natl. Acad. Sci. U. S. A. 107 (2010) 2189–2194.

[20] D. Fukumura, R.K. Jain, Tumor microvasculature and microenvironment: targets for anti-angiogenesis and normalization, Microvasc. Res. 74 (2007) 72–84.

[21] P.P. Hsu, D.M. Sabatini, Cancer cell metabolism: Warburg and beyond, Cell 134 (2008) 703–707.

[22] C.W. Kimbrough, A. Khanal, M. Zeiderman, B.R. Khanal, N.C. Burton, K.M. McMasters, et al., Targeting acidity in pancreatic adenocarcinoma: multispectral optoacoustic tomography detects pH-low insertion peptide probes in vivo, Clin. Cancer Res. 21 (2015) 4576–4585.

[23] M.A. Quadir, S.W. Morton, Z.J. Deng, K.E. Shopsowitz, R.P. Murphy, T.H. Epps, et al., PEG–polypeptide block copolymers as pH-responsive endosome-solubilizing drug nanocarriers, Mol. Pharm. 11 (2014) 2420–2430.

[24] E.C. Dreaden, S.W. Morton, K.E. Shopsowitz, J.-H. Choi, Z.J. Deng, N.-J. Cho, et al., Bimodal tumor-targeting from microenvironment responsive hyaluronan layer-by-layer (LbL) nanoparticles, ACS Nano 8 (2014) 8374–8382.

[25] A.C. Engler, D.K. Bonner, H.G. Buss, E.Y. Cheung, P.T. Hammond, The synthetic tuning of clickable pH responsive cationic polypeptides and block copolypeptides, Soft Matter 7 (2011) 5627–5637.

[26] A. Matsumoto, R. Yoshida, K. Kataoka, Glucose-responsive polymer gel bearing phenylborate derivative as a glucose-sensing moiety operating at the physiological pH, Biomacromolecules 5 (2004) 1038–1045.

[27] J. Rodríguez-Hernández, S. Lecommandoux, Reversible inside – out micellization of pH-responsive and water-soluble vesicles based on polypeptide diblock copolymers, J. Am. Chem. Soc. 127 (2005) 2026–2027.

[28] M. Karaca, R. Dutta, Y. Ozsoy, R.I. Mahato, Micelle mixtures for coadministration of gemcitabine and GDC-0449 to treat pancreatic cancer, Mol. Pharm. 13 (2016) 1822–1832.

[29] D.P. Sanders, K. Fukushima, D.J. Coady, A. Nelson, M. Fujiwara, M. Yasumoto, et al., A simple and efficient synthesis of functionalized cyclic carbonate monomers using a versatile pentafluorophenyl ester intermediate, J. Am. Chem. Soc. 132 (2010) 14724–14726.

[30] J. Liu, W. Liu, I. Weitzhandler, J. Bhattacharyya, X. Li, J. Wang, et al., Ring-opening polymerization of prodrugs: a versatile approach to prepare well-defined drug-loaded nanoparticles, Angew. Chemie Int. Ed. 54 (2015) 1002–1006.

[31] K. Zhou, H. Liu, S. Zhang, X. Huang, Y. Wang, G. Huang, et al., Multicolored pH-tunable and activatable fluorescence nanoplatform responsive to physiologic pH stimuli, J. Am. Chem. Soc. 134 (2012) 7803–7811.

[32] X. Ma, Y. Wang, T. Zhao, Y. Li, L.-C. Su, Z. Wang, et al., Ultra-pH-sensitive nanoprobe library with broad pH tunability and fluorescence emissions, J. Am. Chem. Soc. 136 (2014) 11085–11092.

[33] W. Gao, J.M. Chan, O.C. Farokhzad, pH-responsive nanoparticles for drug delivery, Mol. Pharm. 7 (2010) 1913–1920.

[34] R.M. Carr, M.E. Fernandez-Zapico, Pancreatic cancer microenvironment, to target or not to target? EMBO Mol. Med. 8 (2016) 80–82.

[35] X. Zhang, Y. Lin, R.J. Gillies, J. Nucl. Med. 51 (2010) 1167–1170.

[36] R.J. Gilles, Z. Liu, Z. Bhujwalla, 31P-MRS measurements of extracellular pH of tumors using 3-aminopropylphophonate, Am. J. Physiol. 267 (1994) C195–C203.

[37] V. Estrella, T. Chen, M. Lloyd, J. Wojtkowiak, H.H. Cornell, A. Ibrahim-Hashim, et al., Acidity generated by the tumor microenvironment drives local invasion, Cancer Res. 73 (2013) 1524–1535.

[38] H. Nakashima, M. Nakamura, H. Yamaguchi, N. Yamanaka, T. Akiyoshi, K. Koga, et al., Nuclear factor-kappaB contributes to hedgehog signaling pathway activation through sonic hedgehog induction in pancreatic cancer, Cancer Res. 66 (2006) 7041–7049.

[39] D. Gu, K.E. Schlotman, J. Xie, Deciphering the role of hedgehog signaling in pancreatic cancer, J. Biomed. Res. 30 (2016) 353–360.

[40] A.C. Engler, J.M.W. Chan, D.J. Coady, J.M. O'Brien, H. Sardon, A. Nelson, et al., Accessing new materials through polymerization and modification of a polycarbonate with a pendant activated ester, Macromolecules 46 (2013) 1283–1290.

[41] K. Dan, N. Bose, S. Ghosh, Vesicular assembly and thermo-responsive vesicle-to-micelle transition from an amphiphilic random copolymer, Chem. Commun. 47 (2011) 12491–12493.

[42] D.E. Discher, A. Eisenberg, Polymer vesicles, Science 297 (2002) 967.

[43] J. Du, S.P. Armes, pH-responsive vesicles based on a hydrolytically self-cross-linkable copolymer, J. Am. Chem. Soc. 127 (2005) 12800–12801.

[44] Y. Mai, A. Eisenberg, Self-assembly of block copolymers, Chem. Soc. Rev. 41 (2012) 5969–5985.

[45] K. Kalyanasundaram, J.K. Thomas, Environmental effects on vibronic band intensities in pyrene monomer fluorescence and their application in studies of micellar systems, J. Am. Chem. Soc. 99 (1977) 2039–2044.

[46] Y. Yamamoto, K. Yasugi, A. Harada, Y. Nagasaki, K. Kataokaa, Temperature-related change in the properties relevant to drug delivery of poly(ethylene glycol)–poly (D,L-lactide) block copolymer micelles in aqueous milieu, J. Control. Release 82 (2002) 359–371.

[47] A. Maksimenko, J. Caron, J. Mougin, D. Desmaële, P. Couvreur, Gemcitabine-based therapy for pancreatic cancer using the squalenoyl nucleoside monophosphate nanoassemblies, Int. J. Pharm. 482 (2015) 38–46.

[48] P.M. LoRusso, C.M. Rudin, M.J. Borad, L. Vernillet, W.C. Darbonne, H. Mackey, et al., A first-in-human, first-in-class, phase (ph) I study of systemic Hedgehog (Hh) pathway antagonist, GDC-0449, in patients (pts) with advanced solid tumors, J. Clin. Oncol. 26 (2008) 3516.

[49] S. Sandhiya, G. Melvin, S.S. Kumar, S.A. Dkhar, The dawn of hedgehog inhibitors: Vismodegib, J. Pharmacol. Pharmacother. 4 (2013) 4–7.

[50] E.L. Deer, J. Gonzalez-Hernandez, J.D. Coursen, J.E. Shea, J. Ngatia, C.L. Scaife, et al., Phenotype and genotype of pancreatic cancer cell lines, Pancreas 39 (2010) 425–435.

[51] A. Daemen, D. Peterson, N. Sahu, R. McCord, X. Du, B. Liu, et al., Metabolite profiling stratifies pancreatic ductal adenocarcinomas into subtypes with distinct sensitivities to metabolic inhibitors, Proc. Natl. Acad. Sci. U. S. A. 112 (2015) E4410.

[52] X. Liu, P. Lin, I. Perrett, J. Lin, Y.P. Liao, C.H. Chang, et al., Tumor-penetrating peptide enhances transcytosis of silicasome-based chemotherapy for pancreatic cancer, J. Clin. Invest. 127 (2017) 2007–2018.

[53] K.N. Sugahara, G.B. Braun, T.H. de Mendoza, V.R. Kotamraju, R.P. French, A.M. Lowy, et al., Tumor-penetrating iRGD peptide inhibits metastasis, Mol. Cancer Ther. 14 (2015) 120–128.

[54] M. Loehr, B. Trautmann, M. Goettler, S. Peters, I. Zauner, A. Maier, et al., Expression nad function of receptors for extracellular matrix proteins in human ductal adenocarcinomas of the pancreas, Pancreas 12 (1996) 248–259.

[55] J.H. Lo, L. Hao, M.D. Muzumdar, S. Raghavan, E.J. Kwon, et al., iRGD-guided tumor-penetrating nanocomplexes for therapeutic siRNA delivery to pancreatic cancer, Mol. Cancer Ther. 17 (2018) 2377–2388.